FEM simulations and experimental studies of the temperature field in a large diamond crystal growth cell*

Li Zhan-Chang(李战厂)[a], Jia Xiao-Peng(贾晓鹏)[a], Huang Guo-Feng(黄国锋)[b], Hu Mei-Hua(胡美华)[a], Li Yong(李 勇)[a], Yan Bing-Min(颜丙敏)[a], and Ma Hong-An(马红安)[a]†

[a] *State Key Laboratory of Superhard Materials, Jilin University, Changchun* 130012, *China*
[b] *School of Physics and Electronic Engineering, Chifeng College, Chifeng* 024000, *China*

(Received 1 June 2012; revised manuscript received 15 June 2012)

We investigate the temperature field variation in the growth region of a diamond crystal in a sealed cell during the whole process of crystal growth by using the temperature gradient method (TGM) at high pressure and high temperature (HPHT). We employ both the finite element method (FEM) and *in situ* experiments. Simulation results show that the temperature in the center area of the growth cell continues to decrease during the process of large diamond crystal growth. These results are in good agreement with our experimental data, which demonstrates that the finite element model can successfully predict the temperature field variations in the growth cell. The FEM simulation will be useful to grow larger high-quality diamond crystal by using the TGM. Furthermore, this method will be helpful in designing better cells and improving the growth process of gem-quality diamond crystal.

Keywords: temperature field, finite element method, single crystal growth diamond

PACS: 47.11.Fg, 81.10.Aj, 07.35.+k **DOI:** 10.1088/1674-1056/22/1/014701

1. Introduction

Diamond has been widely used in various fields such as industry, scientific research, national defense, and medical treatment because it has numerous outstanding properties such as high thermal conductivity, the highest hardness, and a wide wave band for light transmission, semiconductor material, etc.[1–5] An increase in the size of single diamond crystals makes the application potential of diamonds more extensive. However, diamonds are now extremely limited in application, because natural diamond resources are extremely limited, especially the larger natural single diamond crystals. Hence, the availability of large synthetic diamonds as an alternative to natural diamonds would greatly broaden the application of diamonds.

The temperature gradient method (TGM) under high pressure and high temperature (HPHT) was developed by the G. E. company in 1971,[1,2] and is still the most effective technique used to grow high-quality gem diamonds.[6–8] When using this method to grow diamonds, it is necessary to regulate the temperature field variations inside the growth cell. According to Ref. [9], without diamond crystal growth in the sealed cell, the temperature remains unchanged within 14 h at the synthesis temperature, as measured by a Pt30%Rh-Pt6%Rh thermocouple. In Ref. [10], after the cell achieved the temperature for diamond synthesis, the author found that the temperature was stable within 1500 s without crystal growth in the cell by means of the finite element method (FEM). However, no one has investigated the variation of temperature field during the crystal growth process in the diamond growth region of the sealed cell. A stable temperature in the cell is indispensable for synthesis of gem-quality diamond crystal by using the TGM. Thus, it is instructive to study the relation between temperature and growth time of synthetic diamonds.

In order to improve the growth process of gem-quality diamond crystal, we require detailed knowledge about the temperature field varying with synthesis time in the growth region of the growth cell. Even though the temperature in the growth region of the growth cell can be investigated experimentally, it is very difficult to characterize the temperature field in the sealed growth cell at HPHT experimentally. The finite element method is a powerful tool for analyzing the growth cell at HPHT. In this paper, we report our application of a China-type cubic anvil high-pressure apparatus, in which large diamond crystals were grown under 5.7 GPa and 1350–1550 °C. The variation of temperature fields during the growth time in the growth region of the growth cell were analyzed by using the FEM and measured by *in situ* experiments. The simulated and experimental results show that the temperature decreases in the process of gem-quality diamond crystal growth. The FEM will be useful for learning how to grow larger high-quality diamond crystals by using the TGM. Furthermore, this method will be effective for cell design and improving the crystal quality of large diamond crystals.

*Project supported by the National Natural Science Foundation of China (Grant Nos. 51071074, 51172089, and 51171070) and the Program for New Century Excellent Talents in University of Ministry of Education of China.

†Corresponding author. E-mail: maha@jlu.edu.cn

© 2013 Chinese Physical Society and IOP Publishing Ltd

2. Computational model and method

2.1. Governing equations of thermoelectricity

The following three-dimensional coupled thermoelectric constitutive equations are dealt with to model the heat transfer in a large diamond crystal growth process that defines the temperature distribution within the growth cell[11]

$$Q = -\nabla \cdot \boldsymbol{q} + \boldsymbol{J}^{\mathrm{T}}\boldsymbol{E} + \rho C\frac{\partial T}{\partial t}, \tag{1}$$

where $\boldsymbol{q}$ is the flux density vector, $\boldsymbol{J}$ is the electric current density vector, $\boldsymbol{E}$ is the voltage vector, ρ is the density, C is specific heat capacity at constant volume, T is the temperature, and t is time.

The thermal field equation in a three-dimensional form is written as

$$q = -\boldsymbol{K}\nabla T, \tag{2}$$

where $\boldsymbol{K}$ is the thermal conductivity matrix. The electric field equation in a three-dimensional form is written as

$$\boldsymbol{J} = \boldsymbol{\delta}\boldsymbol{E}, \tag{3}$$

where $\boldsymbol{\delta}$ is the electric conductivity matrix. The electric field, $\boldsymbol{E}$, can be also expressed by the negative gradient of the potential as

$$\boldsymbol{E} = -\nabla V. \tag{4}$$

Substitution of Eq. (4) into Eq. (3) renders the rate of internal energy generation per unit volume due to Joule heating as a function of the electric potential V only:

$$J = -\delta\nabla V. \tag{5}$$

The coupled equations of thermoelectricity can be obtained from the above equations:

$$Q = \nabla \cdot (K\nabla T) + \sigma\nabla V^2 + \rho C\frac{\partial T}{\partial t}. \tag{6}$$

2.2. Model parameters of diamond growth cell

The experiments of diamond crystal growth were conducted in a China-type cubic anvil high-pressure apparatus. The growth cell is about 10 mm in size. A three-dimensional coupled thermal electrical finite-element simulation on a realistic growth cell is performed. Figure 1(a) shows a cut-away schematic of the finite element model of the diamond growth cell. An enlarged view of the growth cell is shown in Fig. 1(b). Highly pure graphite is used as the carbon source material, which is transformed from graphite phase to diamond before the seed crystal starts to grow. Highly pure nickel is used as a solvent/catalyst. Figure 2 shows the crystal, solvent and carbon source models changing with synthesis time, based on our analysis of experimental data. Optical photos of the crystal and residue of the carbon source after a synthesis experiment lasting 23 h are shown in Fig. 3.

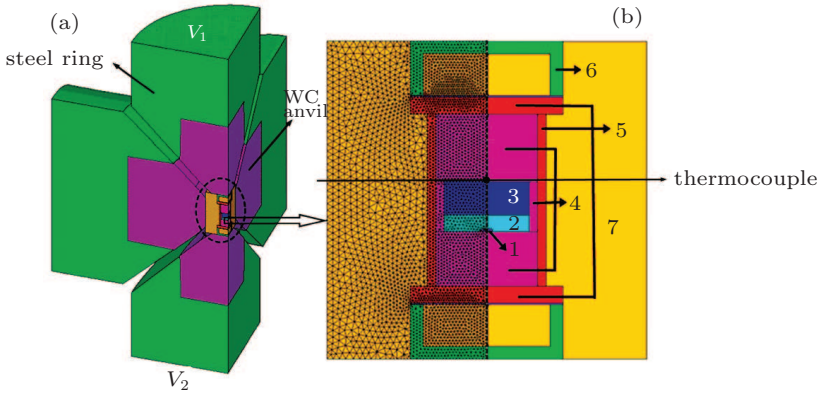


Fig. 1. (color online) Finite element model of a diamond growth cell (a) 1/4 model; (b) enlarged 1/4 growth cell and synthesis assembly. 1: the diamond seed, 2: the solvent, 3: the carbon source, 4: the insulator, 5: the graphite heater, 6: steel cap, 7: the pyrophyllite.

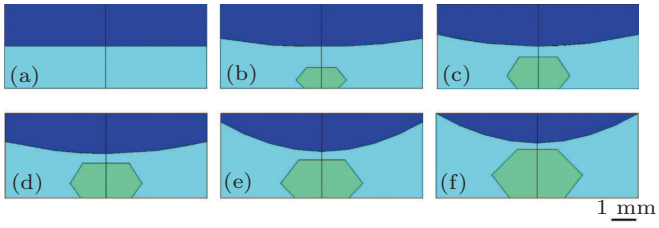


Fig. 2. (color online) Crystal and carbon source model after different synthesis time: (a) 0.5 h; (b) 6.5 h; (c) 1 h; (d) 13 h; (e) 17.5 h; (f) 23 h.

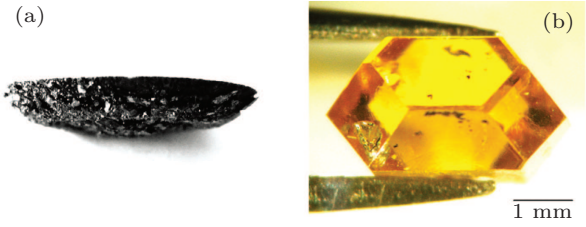


Fig. 3. (color online) Optical photos of (a) remaining carbon source and (b) diamond crystal after a synthesis experiment for 23 h.

2.3. Boundary conditions

The growth experiments of diamond crystals were carried out at 5.7 GPa and 1350–1550 °C. The pressure was estimated by the oil press load, which was calibrated by a curve that is based on the pressure-induced phase transitions of Bi–Ba–Tl. The temperature was measured by inserting a Pt30%Rh-Pt6%Rh thermocouple in the sealed cell (its location is shown in Fig. 1). The growth cell was heated when voltage (2.2 V) is set between the two steel caps which contact a graphite heater and the WC anvils. The bottoms of the six steel rings are kept at a constant temperature of 35 °C.

2.4. Thermo–physical parameters of materials

In order to allow the simulation of temperature fields induced by electric current, we have to determine the main thermo-physical characteristics (ρ, C, δ, λ, etc.) of tested materials. The accuracy of numerical results depends directly on a good evaluation of these parameters. The material parameters used in the finite element simulation are shown in Table 1.[12–26]

Table 1. The material parameters used in the finite element simulation.

Material	Density/kg·m^3	Specific heat/J·kg^{-1}·K^{-1}	Electric resistivity/Ω·m	Thermal conductivity/W·m^{-1}·K^{-1}
Diamond	3510[a)]	471.5[a)]	10^{14}[b)]	470[b)]
Nickel	8900[a)]	460[a)]	1.2×10^{-8} [c)]	19.45+0.0207T[g)]
Graphite	2200[a)]	1000[a)]	$5.21\times10^{-7}+2.95\times10^{-10}T$[c)]	$98384-0.0366T+5.535\times10^{-6}T^2$ [h)]
Pyrophyllite	2950[a)]	800[a)]	2×10^{13}[d)]	4.19+0.39129P[i)]
Steel	7900[a)]	450[a)]	$2.81\times10^{-7}+6.13\times10^{-10}T$[e)]	55.74–0.0241T[j)]
WC	14600[a)]	200[a)]	5.83×10^{-7}[f)]	$94.39-0.038T-7.98\times10^{-6}T^2$[k)]
Insulator (Zirconia)	5600[a)]	450[a)]	8.3×10^{13}[e)]	1.77+4.04$\times10^{-4}T$[l)]

[a)]Ref. [13], [b)] Ref. [14], [c)] Ref. [12], [d)] Ref. [17], [e)] Ref. [19], [f)] Ref. [26], [g)] Ref. [22], [h)] Ref. [23], [i)] Ref. [25], [j)] Ref. [16], [k)] Ref. [15], [l)] Ref. [24].

The growth cell was heated by the Joule heat generated by the electric current passing through the steel rings, the WC anvil, the steel caps, and the graphite heater. For the simulation the temperature-dependent electrical resistivity of steel was set as[16]

$$\delta(T) = 55.74 - 0.0241T \ (\Omega\cdot\mathrm{m}).$$

The electrical resistivity of graphite increases with temperature higher than approximately 400 °C. At high temperature, graphite becomes a better conductor. The temperature-dependent specific electrical resistivity of the graphite heater is approximated by[21]

$$\delta(T) = 5.21\times10^{-7} + 2.95\times10^{-10}T \ (\Omega\cdot\mathrm{m}).$$

The electrical resistivity of WC was set as[26]

$$\delta = 5.83\times10^{-7} \ (\Omega\cdot\mathrm{m}).$$

The simulation results below demonstrate the importance of the thermal conductivities of the assembled materials for determining thermal gradients in a diamond growth cell. The pressure-dependent thermal conductivity of pyrophyllite above 700 °C (see Table tref1).[25] The temperature-dependent thermal conductivities of graphite, insulator, steel, WC, and liquid nickel are shown in Table 1. The thermal conductivity of diamond was set to be 470 W/m·K at 1400 °C and 5.4 GPa[14]

3. Results and discussion

The temperature field distribution in different growth stages during diamond crystal growth is shown in Fig. 4. The results indicate that the temperature distribution continues to change during the process of gem-quality crystal diamond growth. The temperature field distribution at different growth stages of the diamond is uneven. The lower temperature is located in the center of the melted solvent, especially near the surfaces of the crystal. However, the higher temperature is near the insulated tube and carbon source. It can be noticed from the color of the cloud figures that the temperature in the carbon and the crystallization fields of the solvent decreased with diamond crystal growth. Figure 5 shows the temperature distribution in the carbon source along the path indicated by the dashed line in Fig. 4. It can be noticed that the temperature distribution at each growth stage is symmetrical. We can also see that the temperature continues to decrease in the center area of the growth cell as the diamond crystal grows. This phenomenon can be explained by the fact that the diffusion rate of carbon in the process of synthesizing the single crystal diamond is uneven.[27] The diffusion rate of the carbon at the carbon source's edge is faster than at the center. The shape of residual carbon source transforms from a columnar to a spherical cap, as shown in Fig. 3. In addition, as the diamond crystal continues to grow upwards, the crystal face is much closer to the carbon source, and nearly contacts the carbon source. Therefore, the axial thermal diffusivity of the growth cell was strengthened by the carbon diffusivity heterogeneity and diamond single crystal growth.

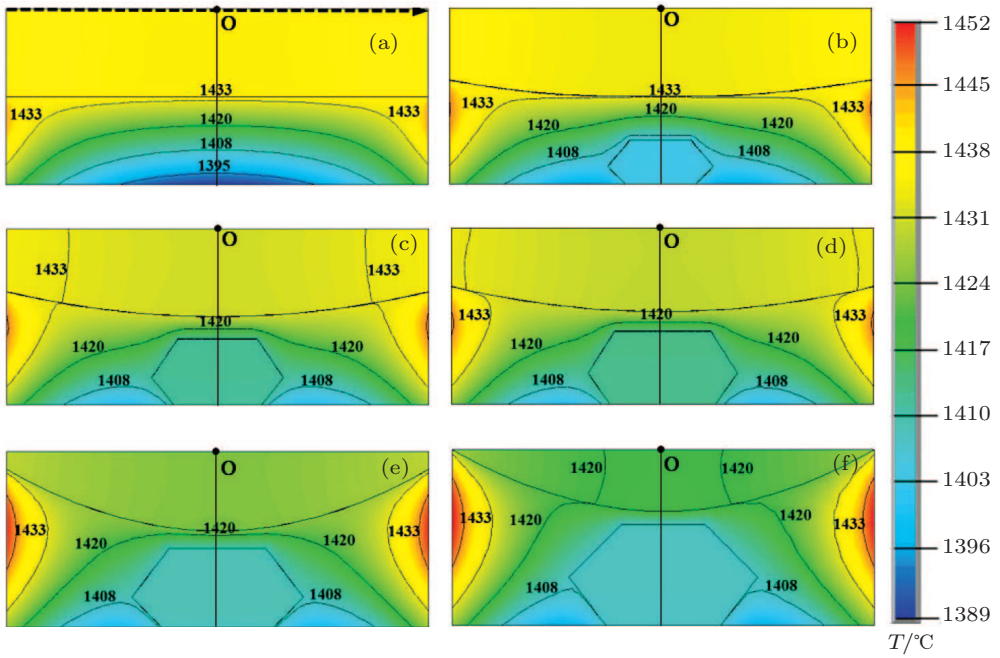


Fig. 4. (color online) Distribution of temperature field in different stages of diamond crystal growth: (a) 0.5 h; (b) 6.5 h; (c) 1 h; (d) 13 h; (e) 17.5 h; (f) 23 h.

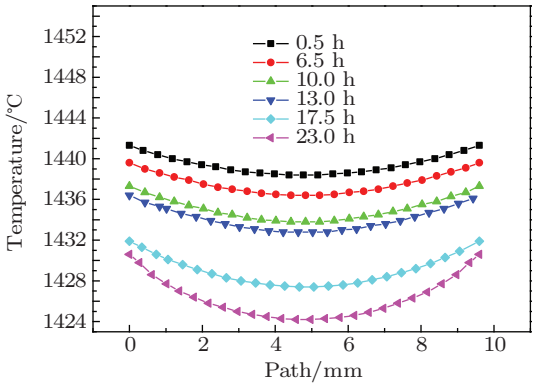


Fig. 5. (color online) Temperature distribution at the top of the carbon source along the path indicated in Fig. 4(a) at different growth times.

From the simulation results above, we have found that the temperature decreased by 15 °C with the growth of the diamond crystal in the center area of the sealed cell for 23 h. It is well known that the growth of diamond crystal requires a stable ambient temperature using the TGM at HPHT. If the ambient temperature changes subtly during the growth process of a large diamond crystal, the quality of the crystal will be influenced significantly. We all know that, in the *P*–*T* phase diagram of carbon (under 5.7 GPa),[28] the region of growing diamond crystal is only a 30-°C range in a V-shaped region bounded by the diamond-graphite equilibrium line and the metal–diamond eutectic line in the solvent–graphite system. In addition, it was reported that the synthesis region of high quality gem diamond crystal has a temperature range of only about 10 °C.[29] The temperature in the crystal growing section decreases during diamond growth. A shift of the crystal synthesis conditions can cause defective crystals and skeleton crystals to form. Therefore, in the growth process of a large diamond crystal, many factors affect the quality of the crystal, such as a temperature decrease in the crystal growth region, solvent/catalyst, cell assembly, ambient humidity, and ambient temperature among which the temperature decrease in the crystal growth region is a primary and crucial factor.

In order to verify our simulation results, we carried out some synthesis experiments at high pressure wherein large diamond crystals were synthesized using a China-type cubic high-pressure apparatus. The cell was heated electrically through a graphite heater, and the temperature was measured by inserting a Pt30%Rh-Pt6%Rh thermocouple in the sealed cell (the location is indicated in Fig. 1). The temperature was measured for 23 h in the experiment. The experimental and simulated results are shown in Fig. 6. It shows that the temperatures measured *in situ* during the experiment decreased by 20.7 °C during the growth of the large diamond crystal in the center area of the growth cell. The experimental results show that there are two distinct stages during the diamond crystal growth: an initial stage that lasts 5 h and a late stage that continues from 5 to 23 h. In the initial stage, the phase transition of the pressure-transmitting medium and the material of the synthesis assembly are compressed, which leads to a rapid change of material parameters and temperature. In the late stage, since the material of the synthesis assembly is relatively stable, the temperature changes slowly, which is similar to that of our simulation results. From the simulated and measured results above, we have found that the temperature in the center of the growth region decreases as the gem diamond crystal grows. Despite of the discrepancy between the simulation

results and the experimental results, the simulated results are fundamentally in very good agreement with the experimental data. Therefore, the finite element model can successfully predict the temperature field variations during the gem diamond crystal growth.

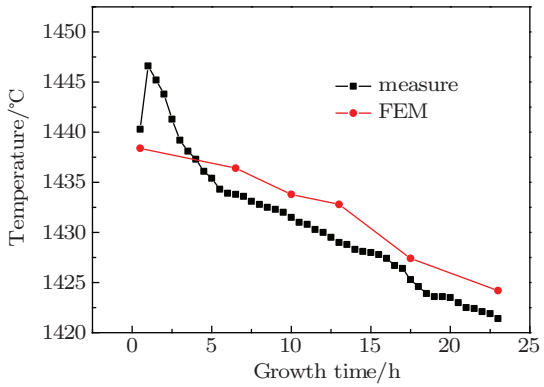


Fig. 6. (color online) Comparison of measured and simulated temperature variation in the center point (indicated by O in Fig. 4) of the growth cell.

4. Conclusions

The temperature field variation during the diamond growth process was investigated by using the FEM simulation and *in situ* experiments. The simulation results show that the temperature continues to decrease as the diamond crystal grows in the center area of the growth cell. The results are in good agreement with the experimental data, which demonstrates that the finite element model can successfully predict the temperature field variation in the growth cell. The FEM simulation will be useful for learning how to grow larger high-quality diamond crystal by using the TGM. Furthermore, this method can be employed to design growth cells and is useful for improving the growth process of gem-quality diamond crystal.

References

[1] Strong H M and Chrenko R M 1971 *J. Phys. Chem.* **75** 1838
[2] Wentrof R H 1971 *J. Phys. Chem.* **75** 1833
[3] Li S S Ma H A, Li X L, Su C, Jia X P, Ma H A, Huang G F and Li Y 2011 *Chin. Phys.* B **20** 028103
[4] Yoder M N 1991 *Diamond and Diamond-Like Films and Coatings* (New York: Plenum Press)
[5] Isoya J, Kanda H and Akaishi M 1997 *Diamond and Related Materials* **6** 356
[6] Li Y, Jia X P, Hu M H, Liu X B, Yan B M, Zhou Z X, Zhang Z F and Ma H A 2012 *Chin. Phys.* B **21** 058101
[7] Huang G F, Jia X P, Li Y, Hu M H, Li Z C, Yan B M and Ma H A 2011 *Chin. Phys.* B **20** 078103
[8] Huang G F, Jia X P, Li S S, Zhang Y F, Li Y, Zhao M and Ma H A 2010 *Chin. Phys.* B **19** 118101
[9] Huang G F 2008 *Growth of Type Ib Diamond Crystal with Multi-Seed Under High Temperature and High Pressure by Temperature Gradient* (MS. thesis) (Changchun: Jilin University) (in Chinese)
[10] Li R, Ma H A and Hang Q G 2008 *Journal of Jilin University (Engineering and Technology Edition)* **38** 535 (in Chinese)
[11] Zhai F G, Sun T and Ren W B 2009 *Chin. Soc. Elec. Eng.* **29** 118 (in Chinese)
[12] ASM Handbook 1990 *Properties and Selection: Nonferrous Alloys and Special-Purpose Materials* (vol. 2) (ASM International)
[13] Ma Q F 1986 *Practical Handbook of Thermal Physical Properties* (Beijing: China Agricultural Machinery Press) (in Chinese)
[14] Nazare M H and Neves A J 2001 *Properties, growth, and Applications of Diamond* (EMIS Datareview series No. 26) (INSPEC: Institution of Electrical Engineers)
[15] Emelyanov A E 1994 *High Temperatures-High Pressures* **15** 663
[16] Zhang J R and Zhao T Y 1987 *Handbook of Thermo-Physical Parameter for Usual Used Material in Engineering* (Beijing: New Times Press) (in Chinese)
[17] Hicks T L and Secco R 1997 *Can. J. Earth Sci.* **34** 875
[18] Dawson D K and Creamer R H 1965 *Br. J. Appl. Phys.* **16** 1643
[19] Lide D R 1995 *Handbook of Chemistry and of Physics* (75th edn.) (London: The Chemical Rubber Co.)
[20] Rothman M F 1988 *High-Temperature Property Data: Ferrous Alloys* (ASM International, Materials Park)
[21] Pierson H O 1994 *Handbook of Carbon, Graphite, Diamond, and Fullerenes* (Park Ridge: Noyes Publications)
[22] Nishi T, Shibata H, Ohta H and Waseda Y 2003 *Met. Mat. Trans.* A **34A** 2801
[23] Taylor R E, Davis F E and Powell R W 1969 *High Temperatures-High Pressures* **1** 663
[24] Kingery W D, Francl J, Coble R L and Vasilos T 1954 *J. Am Ceram. Soc.* **37** 107
[25] He S A, Li J L and Cheng X R 1977 *Acta Phys. Sin.* **2** 100 (in Chinese)
[26] Pierson H O 1999 *Handbook of Chemical Vapor Deposition: Principles, Technology and Applications* (2nd edn.) (Norwich: Noyes/William Andrew)
[27] Zang C Y, Ma H A, Li R and Li S S 2008 *Superhard Mater. Eng.* **20** 11 (in Chinese)
[28] Strong H M and Hanneman R E 1967 *J. Phys. Chem.* **46** 3668
[29] Sumiya H Toda N and Satoh S 2002 *J. Cryst. Growth* **337** 1281